Electric Power Systems Research 129 (2015) 142–149

Contents lists available at ScienceDirect

Electric Power Systems Research

journal homepage: www.elsevier.com/locate/epsr

Accurate reactive power control of autonomous microgrids using an adaptive virtual inductance loop

Ramin Moslemi, Javad Mohammadpour*

Complex Systems Control Lab, College of Engineering, The University of Georgia, Athens, GA 30602, United States

ARTICLE INFO

Article history:
Received 3 April 2015
Received in revised form 17 July 2015
Accepted 4 August 2015

Keywords:
Autonomous microgrids
Reactive power sharing
Output virtual impedance

ABSTRACT

In this paper, a new droop-based reactive power control strategy is proposed that is suitable for implementation in autonomous low voltage microgrids. The proposed method exploits the potentials of adding a dynamic virtual inductance loop to compensate for the voltage drop differences caused by line impedances. In addition, it provides a large virtual inductance at the output terminals of a distributed generation (DG) source to eliminate the coupling between the active and reactive powers. Finally, the efficiency of the proposed method to cope with the aforedescribed challenges is examined using comprehensive simulation studies.

1. Introduction

In the last decade, incremental public concerns about environmental issues, persistent growth in the power demands and the need for more efficient and reliable power grids have led to fundamental changes in the power industry. This is done to move towards accommodating higher levels of renewable energy sources (RESs) in the form of distributed generations (DGs) [1]. Relentless increase in the penetration of distributed generations in power distribution networks has initiated the concept of *microgrid*. As described in Ref. [2], a region with enough energy supplies to operate autonomously when it becomes disconnected from the rest of grid could be considered as a microgrid. The microgrids are able to operate in both grid-connected and autonomous (also known as islanded) modes. In autonomous mode, a DG inverter operates like a voltage source and the microgrid dynamics is highly dependent on the connected DGs and the power regulation controls.

A wide variety of methods have been proposed in the literature in order to offer a plug and play capability for DERs. Although communication-based approaches such as master and slave and distributed control (see, e.g.,[3] and the references therein), can provide accurate power sharing control, any failure in master unit or data exchange communication links could bring about whole or partial shut down in the microgrid. Therefore, the decentralized control designs are preferred [4]. However, communication could still be used in higher levels of hierarchical structure of microgrids to control slower dynamics and optimize the operation of autonomous microgrids. Losing communication links, in this architecture, would compromise optimality of the operation; however, the microgrid would still continue to provide power service [5]. Therefore, among the proposed control approaches, a decentralized control, known as droop control, has attracted a lot of attention due to its simplicity and redundancy [6].

Very early droop control techniques were proposed assuming decoupled active and reactive powers in predominantly inductive lines [7]. However, this assumption is not valid for medium or low voltage microgrids, in which the feeders have mixed or even resistive impedances, respectively. To avoid the coupling between active and reactive powers, virtual impedance methods have been proposed to make inverters output impedance highly inductive [8]. The main problem in using virtual impedance method is that the reactive power sharing may exacerbate because of an increase in impedance voltage drops.

As an objective of a plug and play configuration, the active and reactive powers should be shared accurately and proportionally among the DGs. The active power-frequency droop can realize accurate active power sharing [9]. On the other hand, the reactive power sharing accuracy is affected by voltage differences at the inverters' output terminals. To share linear or nonlinear reactive loads in a distributed AC power system, a new approach was proposed in [10] by introducing additional control inputs. However, by applying this method, the line currents may be distorted because of an increase in controller complexity. In Ref. [11], a modified version of voltage and reactive power droop was introduced to compensate

* Corresponding author. Tel. +1 7065427295.
E-mail address: javadm@uga.edu (J. Mohammadpour).

http://dx.doi.org/10.1016/j.epsr.2015.08.001
0378-7796/

for the effect of voltage drops caused by feeder impedances through modifying the droop slopes. Although the suggested method could achieve a more accurate reactive power sharing, it would need an online slope estimation, which makes this strategy quite complicated.

In microgrids with several DG inverters operating in parallel, the difference between inverters' output voltages causes circulating current among inverters. The circulating current may lead to inverters overcurrent and also a degradation in droop control efficiency. A modified virtual impedance approach was presented in [12] to mitigate the circulating current among inverters, but the proposed approach could be used only for DGs with the same rating. Furthermore, the method proposed in Ref. [12] could not cope with reactive power sharing problem because of the voltage differences at the outputs of inverters.

In this paper, a new variable virtual inductance control loop, along with a modified energy management system (EMS), is proposed to enhance the performance of the traditional droop controllers to simultaneously cope with the following problems: (1) eliminating active and reactive power coupling in low and medium voltage microgrids; (2) achieving an accurate proportional reactive power sharing; (3) mitigating the circulating current among inverters, without the need for communication between DG units in the primary level.

The remainder of this paper is organized as follows. In Section 2, the principle of conventional droop method is explained and its drawbacks are reviewed. In Section 3, the proposed modified virtual impedance control loop is elaborated to address the conventional droop control issues. In Section 4, simulation results will be presented and the efficiency of the proposed droop control will be evaluated, and finally Section 5 concludes the paper.

2. Traditional droop control technique

The ability to control the inverter output voltage is one of the best ways to realize DG plug and play feature in autonomous microgrids. The droop control method has been devised based on the power flow equations between voltage sources separated by a line impedance given as [7]

$$P_{12} = \frac{E_1}{R^2+X^2}[R(E_1 - E_2\cos\delta) + XE_2\sin\delta] \quad (1)$$

$$Q_{12} = \frac{E_1}{R^2+X^2}[X(E_1 - E_2\cos\delta) - RE_2\sin\delta] \quad (2)$$

where E_1 is the voltage magnitude of the inverter output, E_2 is the bus voltage magnitude, X and R are line inductance and resistance, respectively, and δ is the angle difference between E_1 and E_2. Also, P_{12} and Q_{12} represent active and reactive powers injected by the inverter to the transmission line. Neglecting the line resistance and assuming the phase angle to be sufficiently small, the above equations could be simplified, where the active and reactive powers would be proportional to the phase angle difference δ and the voltage magnitude difference $(E_1 - E_2)$, respectively. Based on these relationships, in autonomous mode, the DG active power can be controlled with changing output voltage frequency and the reactive power can be regulated by modifying DG output voltage magnitude difference. Therefore, the conventional droop control for the microgrids with highly inductive lines takes the following form

$$\omega_i = \omega^* - M_{P_i}(P_i^* - P_i) \quad (3)$$

$$E_i = E^* - M_{Q_i}(Q_i^* - Q_i), \quad (4)$$

where P_i and Q_i are active and reactive power outputs of ith DG, respectively, P_i^* and Q_i^* are the ith DG dispatched powers in the grid-connected mode, ω^* and E^* are frequency and voltage magnitude at the grid-connected mode and M_{P_i}, M_{Q_i} are frequency and voltage droop slopes, respectively. Since it is preferred to make each DG generate active and reactive powers in proportion to its power capacity, the droop slopes are defined as

$$M_{P_i} = \frac{\omega^* - \omega^{\min}}{P_i^* - P_i^{\max}} \quad \text{and} \quad M_{Q_i} = \frac{E_i^* - E^{\min}}{Q_i^* - Q_i^{\max}}, \quad (5)$$

where $P_i^{\max}$ and $Q_i^{\max}$ are the maximum active and reactive power outputs, and $\omega^{\min}$ and $E^{\min}$ are minimum allowable operating frequency and voltage, respectively. Although the droop control strategy is easy to implement due to its simplicity and is also reliable due to its decentralized structure, the conventional droop controllers suffer from several drawbacks reviewed in following section.

2.1. Drawbacks of the conventional droop control methods

As mentioned earlier, the $P-\omega$ and $Q-E$ droops are derived based on the assumption that the lines are highly inductive. This is indeed a valid assumption for conventional power systems with long distance transmission lines; however, in the medium and low voltage (LV) microgrids, the lines and distribution feeders are mixed impedance or even dominantly resistive that introduces a significant coupling between the active and reactive power flows especially during transients. Therefore, the transient response of the conventional droop methods becomes poor [13], especially in LV microgrids. To address this problem in LV microgrids, a large inductance could be added to the output impedance of DGs. The traditional virtual impedance techniques realize this solution by adding a large virtual inductance at the DG output; however, employing virtual impedance could increase the reactive power sharing inaccuracy because of the voltage drops due to the added virtual inductance.

An accurate active power sharing could be easily realized, whereas obtaining an accurate reactive power sharing among inverters is a challenging task due to the difference in voltage magnitude at the DGs output voltages. Fig. 1a shows the schematic of a small microgrid with two DGs that supply active and reactive power to a sensitive load. The $Q-E$ droop works based on the voltage difference between the point of common coupling (PCC) and the DG output to allow an appropriate reactive power flow. For a highly inductive line, the voltage drop on line impedance, i.e., voltage magnitude difference between the DG output voltage and PCC voltage, could be approximated as a linear function of the DG output reactive power by

$$\Delta E_i = E_i - E_{\mathrm{PCC}} \simeq \frac{X_i \times Q_i}{E_i}. \quad (6)$$

Therefore, due to the difference in line impedances or in currents flowing from DGs to the load, the voltage drops on the line impedances will be different. As a result, the DGs output voltages would be different that leads to reactive power sharing errors. Fig. 1b shows an inaccuracy in the reactive power when conventional droop methods are applied for voltage regulation. By considering (6), when the microgrid is fully loaded (voltage at PCC is at minimum acceptable value $E_{\mathrm{PCC}}^{\min}$), DG1 and DG2 operate at points (E_1,Q_1) and (E_2,Q_2), respectively, as seen in Fig. 1b. Therefore, the first unit operates below the minimum acceptable voltage ($E_1^{\min}$) and generates a reactive power higher than its maximum power output ($Q_1^{\max}$), while second DG provides lower than its maximum reactive power ($Q_2^{\max}$), hence violating reactive power sharing requirements. This could lead the DG system to exceed current ratings and hence unacceptable voltage drops (less than $E^{\min}$) at sensitive load buses [11].

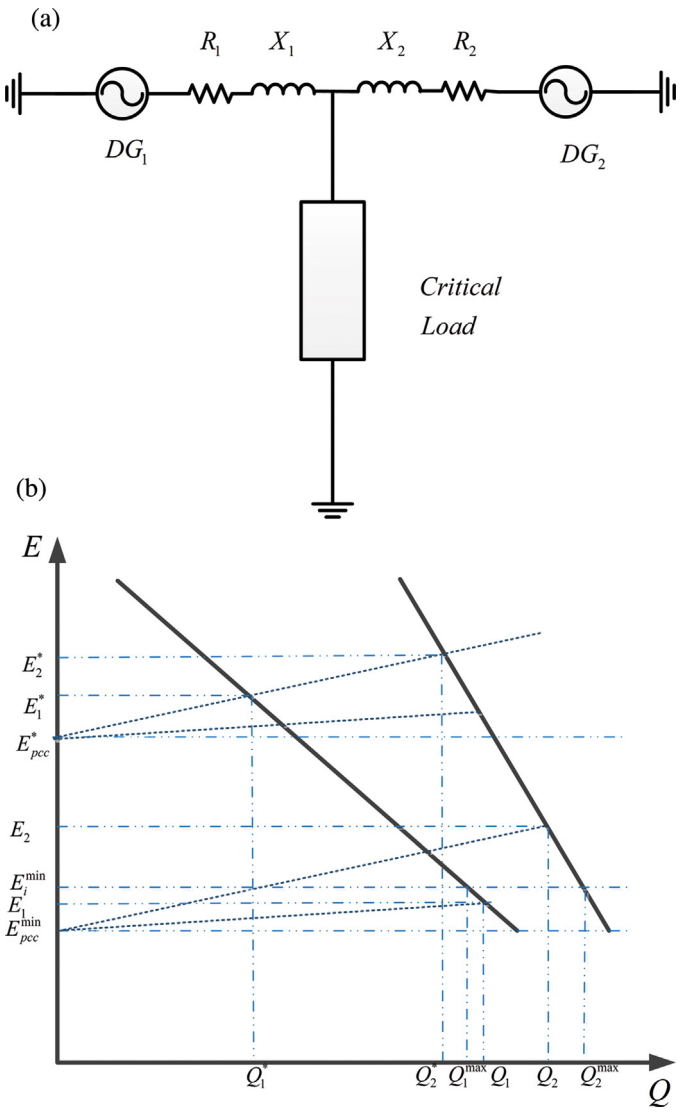

Fig. 1. (a) Two voltage source inverters (VSIs) operate in parallel to supply a critical load, (b) the effect of line inductance in reactive power sharing accuracy for two inverters operating in parallel.

In addition to reactive power sharing inaccuracy, different output voltages of DGs can result in circulating currents among inverters that reduce the efficiency of droop controller and also cause inverters overcurrent in the microgrids. The circulating current for two inverters that supply a common load can be obtained by doing simple circuit analysis and applying some simplifications as [12]

$$\Delta\bar{I} = \frac{\bar{I}_1 - \bar{I}_2}{2} = \frac{\bar{I}_{p1} - \bar{I}_{p2}}{2} + j\frac{\bar{I}_{q1} - \bar{I}_{q2}}{2} = \Delta\bar{I}_p + j\Delta\bar{I}_q \tag{7}$$

where $\Delta\bar{I}$ is the circulating current and $\Delta\bar{I}_p$ and $\Delta\bar{I}_q$ are the active and reactive components of the circulating current, respectively. To simplify the calculation of the active and reactive components, it is assumed that both lines have the same impedances. It is then straightforward to obtain

$$\Delta\bar{I}_p = \frac{1}{2} \times \frac{R_1(E_1 - E_2)}{R_1^2 + (\omega L_1)^2} \quad \text{and} \quad \Delta\bar{I}_q = \frac{1}{2} \times \frac{\omega L_1(E_1 - E_2)}{R_1^2 + (\omega L_1)^2} \tag{8}$$

where ω is the operating frequency, R_1 and L_1 are resistance and reactance of the transmission lines and E_1 and E_2 are the DGs' output voltages, respectively. As (8) illustrates, the circulating current is generated because of the voltage differences between inverters' output voltages caused by parameters mismatch. Although designing an appropriate traditional virtual impedance could reduce circulating current among DGs to some extent [12], the most effective way to eliminate it is by minimizing the output voltage differences between the inverters.

3. Improved droop control using virtual impedance

Virtual impedance methods were originally introduced in microgrid applications in order to eliminate $P-Q$ coupling in LV microgrids, where the grid interactive uninterruptible power supplies (UPS) are connected directly to PCC with resistive feeders [14]. If designed properly, the virtual inductance could also improve power sharing by reducing the sensitivity of power sharing to the output impedance. In addition, the virtual impedance could be used in order to improve the transient response of microgrids that is highly oscillatory due to the poor inertia of autonomous microgrids. To maximize the benefits of virtual impedance, the impedance value should be chosen appropriately and the virtual impedance scheme should be modified to achieve desired design specifications [15]. In most virtual impedance applications, the added impedance is a pure inductance to make the output impedance highly inductive; however, this concept could be extended to mix impedance in order to satisfy some specific requirements. In conventional virtual impedance control loops, in order to mimic the behavior of an impedance, the line current is fed back. Then, the feedback signal is differentiated and multiplied by desired inductance value as

$$\Delta V = L_{vir} \times \frac{di_{inv}}{dt} \tag{9}$$

where ΔV is the voltage magnitude drop caused by the virtual impedance, L_{vir} is the desired virtual inductance and i_{inv} is the inverter output current. Then, the obtained voltage drop is subtracted from the voltage reference generated by primary controller (here, droop controller) to imitate the behavior of real inductance located exactly at the output of inverter. The differentiation of line current makes the virtual impedance control loop very sensitive to high frequency harmonics of the line current. To prevent amplification of noise existing in the line current, the authors in Ref. [16] implemented a high-pass filter to bound the high frequency noise on the virtual impedance output.

3.1. Proposed adaptive virtual impedance

The proposed virtual impedance architectures in the literature have addressed specific problems to some extent, but their applications have been restricted to a single control requirement, e.g., eliminating active and reactive power coupling. Also, the conventional virtual impedance methods proposed for reactive power sharing can only be applied to microgrids with identical DGs, and the efficiency of these approaches is highly dependent on the detailed knowledge of the system parameters and the accuracy of the design.

Although it is desired to achieve a fast dynamic response by employing decentralized controllers, the design of a centralized controller should still be considered. Centralized controller can be utilized at a higher level with slower dynamics for real-time optimization and frequent adjustment of microgrids and DG parameters to minimize costs or meet other targets [17]. Therefore, energy management systems (EMS) have been proposed in modern microgrids as a centralized controller with a larger time constant compared to droop controllers to allow these functionalities [18]. EMS updates the droop controller parameters at every time intervals (several minutes) based on the optimal power flow results, security measures and other considerations. The method presented

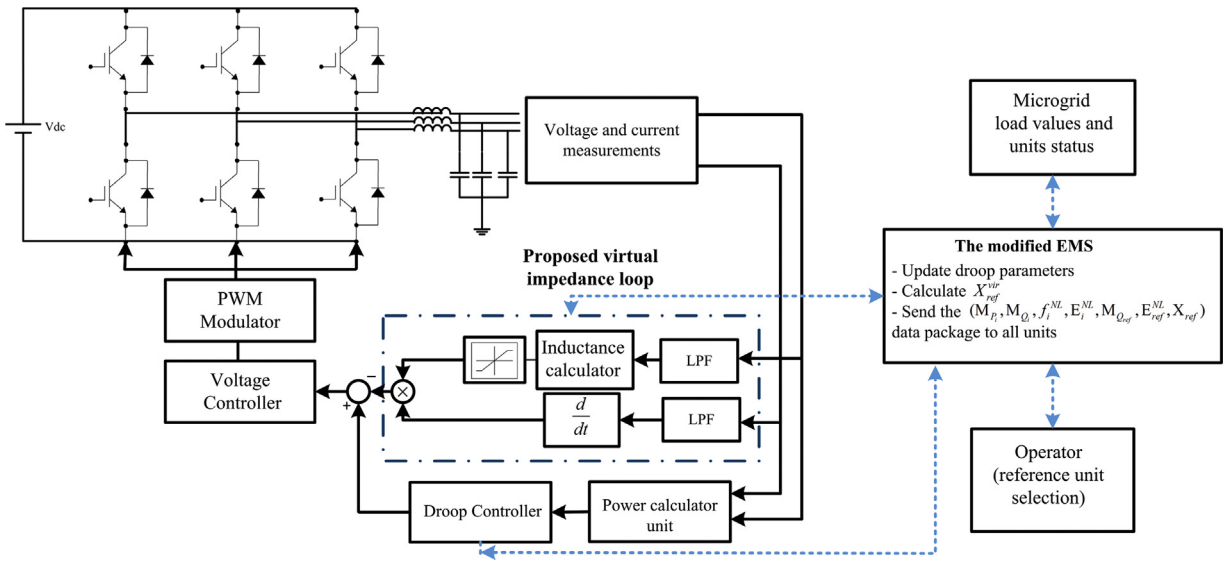

Fig. 2. Proposed adaptive virtual impedance with a voltage control scheme for the DG interfacing inverter.

in this paper exploits the potential of existing EMS structure to send some critical information to all DGs and update this information at each EMS time interval. It should be noted that the communication links used for EMS are low band, cheap and already existing in modern grids.

The main idea behind the proposed method is to implement a time-varying virtual impedance to enable all DGs to coordinate their output voltage with the estimated output voltage of a reference DG through changing their output virtual impedances. To clarify this point, consider for the microgrid with two parallel DGs that supply power to a critical load at PCC (Fig. 1a) that one of the DGs is selected as the reference unit. It is desired to eliminate the voltage differences between the output of inverters, i.e.,

$$E_i = E_{\text{ref}} \Rightarrow E_i - E_{\text{PCC}} = E_{ref} - E_{\text{PCC}} \Rightarrow \Delta E_i = \Delta E_{\text{ref}}$$

where E_{ref} is the output voltage of the reference unit and E_{PCC} is the voltage at the PCC. Considering the above condition, Eqs. (4), (6), Fig. 1b and assuming that lines are highly inductive, because of the virtual impedance loop, the value of the DG output inductance can be obtained as

$$X_i = X_{\text{ref}} \times \frac{Q_{\text{ref}}}{Q_i} \tag{10}$$

where Q_{ref} is the output reactive power of the reference unit, Q_i is the reactive power of the ith DG, $X_{\text{ref}} = X_{\text{ref}}^{\text{line}} + X_{\text{ref}}^{\text{vir}}$ and $X_i = X_i^{\text{line}} + X_i^{\text{vir}}$, where X_i^{line} is the DG line inductance and X_i^{vir} is the DG virtual inductance value. Also, it is important to note that lines' impedances could be estimated accurately by employing standard estimation methods either offline or in real time [19].

The nature of the droop control method requires that the controller relies only on the local measurements. Therefore, the proposed method, instead of using real time measurements of reference unit output, only estimates the value of reactive power generated at the reference unit to adjust its virtual impedance. The droop parameters of the reference DG updated by EMS unit at each update interval (and sent to all DGs) are utilized to estimate the desired virtual inductance between the ith DG (X_i^{vir}) that could compensate for the voltage differences at the output of ith DG and the reference one. Using (10) and comparing the reactive power droop equations (4) for the units leads to

$$X_i^{\text{vir}} = X_{\text{ref}} \times \frac{E_{\text{ref}}^{\text{NL}} - E_i}{E_i^{\text{NL}} - E_i} \times \frac{M_{Q_i}}{M_{Q_{\text{ref}}}} - X_i^{\text{line}} \tag{11}$$

where E_i^{NL} and $E_{\text{ref}}^{\text{NL}}$ are the ith and reference no-load output voltages, respectively. All the parameters in the above equation are available for the inverters' local controllers and updated at each interval by the modified EMS. Using the above equations, the structure to realize the proposed method is as follows:

Highest level: In this level the reference DG unit is selected. All other inverters will have to track the output voltage of this unit. Different criteria could be used to select the reference unit. Because of the reliability concerns, the DG with minimum changes in the droop parameters is selected as the reference DG. It is noted that at each grid, there are some units that operate with almost constant operating points (Q_i^*, M_{Q_i}) because of economical or security considerations. Also, it is worth noting that the proposed method is very flexible and the reference unit could be changed at any EMS update interval to ensure prescribed specifications.

EMS level: The EMS updates the droop parameters and operating points of all DGs based on the economical and security requirements. It then calculates the value of virtual impedance at the reference bus by applying (4) and (6) such that when the voltage at PCC (E_{PCC}) is at its minimum, the DG generates its maximum reactive power ($Q_{\text{ref}}^{\max}$) at the minimum acceptable output voltage ($E_i^{\min}$). Therefore, all units provide their maximum reactive powers when the PCC is at lowest acceptable point. Then, the updated droop parameters of each DG, updated values of reference DG parameters and its virtual impedance are sent to all DGs. As a result, after each update interval, all units would have received their updated droop values, as well as the reference DG droop parameters and its virtual impedance value.

Primary level: To imitate the behavior of a variable inductor, the line current and voltage are fed back to calculate the desired dynamic voltage drop due to applying the proposed virtual inductance loop. Both current and voltage signals pass through low pass filters to suppress the high frequency noise at the output current and also to make the adaptive virtual impedance loop slower than the $Q-E$ loop. Then, the voltage feedback signal is used to

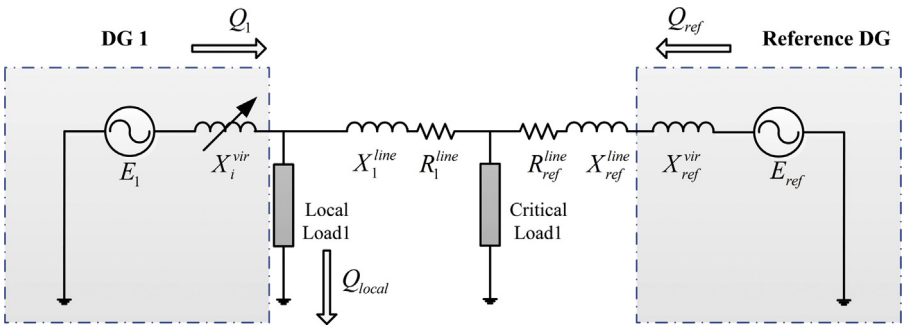

Fig. 3. A microgrid with a local load and two parallel inverters.

determine the value of desired virtual inductance (X_i^{vir}) by applying (11). In the next step, the obtained X_i^{vir} and the derivative of inverter output current are used to generate the reference signal and voltage drop on the virtual inductor. This voltage drop is subtracted from the voltage reference generated by the reactive power droop control loop to calculate final voltage reference that should be tracked by the voltage controller.

Fig. 2 shows the structure of the proposed adaptive virtual impedance and its interface with the reactive power droop and voltage control loop. The average feedback linearization control method is employed here instead of cascade voltage and current controllers for each phase of inverter. This is to linearize, in a large-signal sense, and attain accurate voltage tracking of the output voltage. The details about average feedback linearization controller can be found in [8]. It is worth noting that the saturation has also been applied in the virtual impedance loop to keep the virtual inductance within an acceptable range from the stability and operation points of view.

3.2. Compensation of local load impact using an enhanced adaptive virtual impedance

The approach presented in the previous section can achieve almost zero voltage drop differences when several DGs operate in parallel to supply one critical load. But in actual multi-bus microgrids, usually some of the DGs supply power to local loads directly connected to them. Location and the amount of local loads can cause changes in the power flows and as the result affect the reactive power sharing accuracy [11]. In this section, we describe the modification made to the proposed virtual impedance method to cope with the local load effects on DGs, output voltages and reactive power sharing accuracy.

Fig. 3 shows a microgrid with two DGs, in which the first unit has a local load located directly at the DG output and the second DG is considered as the reference unit. The DGs have been modeled as voltage sources connected to the inductors at their outputs. The inductors model the virtual impedance loops; hence, the DG1 inductance (X_1^{vir}) is considered to be varying (adaptive virtual impedance loop), while the second DG inductance is constant. Our enhanced adaptive virtual impedance loop is utilized here to achieve equal voltage magnitudes at the output of DGs droop controller, i.e., voltage sources outputs in equivalent model E_1 and E_{ref}. This could be realized if

$$\Delta E_1^{\text{vir}} + \Delta E_1^{\text{line}} = \Delta E_{\text{ref}}^{\text{vir}} + \Delta E_{\text{ref}}^{\text{line}} \tag{12}$$

where ΔE_1^{vir}, $\Delta E_{\text{ref}}^{\text{vir}}$ are voltage drops across the virtual impedances of DG1 and the reference DG, respectively, and ΔE_1^{line} and $\Delta E_{\text{ref}}^{\text{line}}$ represent the voltage drops caused by DG1 and the reference DG lines' inductances, respectively. Neglecting the voltage drop caused by the line resistances and using (6), Eq. (12) can be rewritten as

$$\frac{Q_1 \times X_1^{\text{vir}}}{E_1} + \frac{(Q_1 - Q_{\text{local}}) \times X_1^{\text{line}}}{(Q_1 \times X_1^{\text{vir}})/E_1} = \frac{Q_{\text{ref}} \times (X_{\text{ref}}^{\text{vir}} + X_{\text{ref}}^{\text{line}})}{E_{\text{ref}}} \tag{13}$$

where Q_1 and Q_{ref} are reactive powers generated by DG1 and the reference DG, respectively, and Q_{local} is the reactive local load connected to DG1. Also, E_1 and E_{ref} denote the voltage references created by the droop controllers of DG1 and the reference DG, respectively. Using droop Eq. (4) and considering $E_1 = E_{\text{ref}}$, the reactive power generated by the reference unit can be estimated as

$$Q_{\text{ref}} = \frac{E_{\text{ref}}^{\text{NL}} - E_1}{E_1^{\text{NL}} - E_1} \times \frac{M_{Q_1}}{M_{Q_{\text{ref}}}} \times Q_1 \tag{14}$$

Substituting (14) into (13) and solving the obtained equation, which is quadratic in X_1^{vir}, results in

$$X_1^{\text{vir}} = \frac{E_1^2}{2Q_1} \times [1 + \beta X_{\text{ref}}^t \frac{Q_1}{E_1^2} \pm \sqrt{(1 + \beta X_{\text{ref}}^t \frac{Q_1}{E_1^2})^2 - \frac{4Q_1}{E_1^2}((\alpha - 1)X_1 + \beta X_{\text{ref}}^t)}] \tag{15}$$

where $X_{\text{ref}}^t = X_{\text{ref}}^{\text{vir}} + X_{\text{ref}}^{line}$, $\alpha = Q_{\text{local}}/Q_1$ and $\beta = Q_{\text{ref}}/Q_1$. The X_1^{vir} obtained from (15) guarantees an accurate reactive power sharing among inverters. As indicated by (15), the proposed approach modifies the value of virtual inductance only based on the local measurements and the reference droop parameters sent to the DGs at every EMS update interval. The proposed approach could be readily extended to microgrids with more than two DGs and local loads. It is worth noting that both values obtained for X_1^{vir} in (15) satisfy the equal voltage magnitude requirement, but to prevent abnormal voltage drop at the DGs' output, the value closer to the reference unit inductance ($X_{\text{ref}}^{\text{vir}}$) may be selected. Also, the proposed method will reduce the circulating current among inverters as well because the voltage magnitudes at the output of droop controllers are almost the same, i.e., $E_1 = E_2 = \ldots = E_{\text{ref}}$ (voltage drop caused by active powers and line resistances is neglected).

4. Simulation results and discussion

To validate the efficacy of the proposed approaches in coping with the aforementioned droop control challenges, a microgrid with two DGs operating in parallel(parameters are presented in Table 1), has been simulated in MATLAB/Simulink®. The DGs' reactive power droop parameters have been selected to be unequal intentionally to highlight the flexibility of the proposed virtual impedance loop. The second DG has been selected as the reference unit while the first one adjusts its operating point based on the reference DG droop parameters.

In the first simulation, it is assumed that there is no local load and both DGs supply active and reactive powers to a critical load located at PCC. Firstly, both DGs are assumed to use conventional virtual impedance. The values of virtual reactances for both DGs are considered to be 2 mH to introduce high inductance at the outputs of

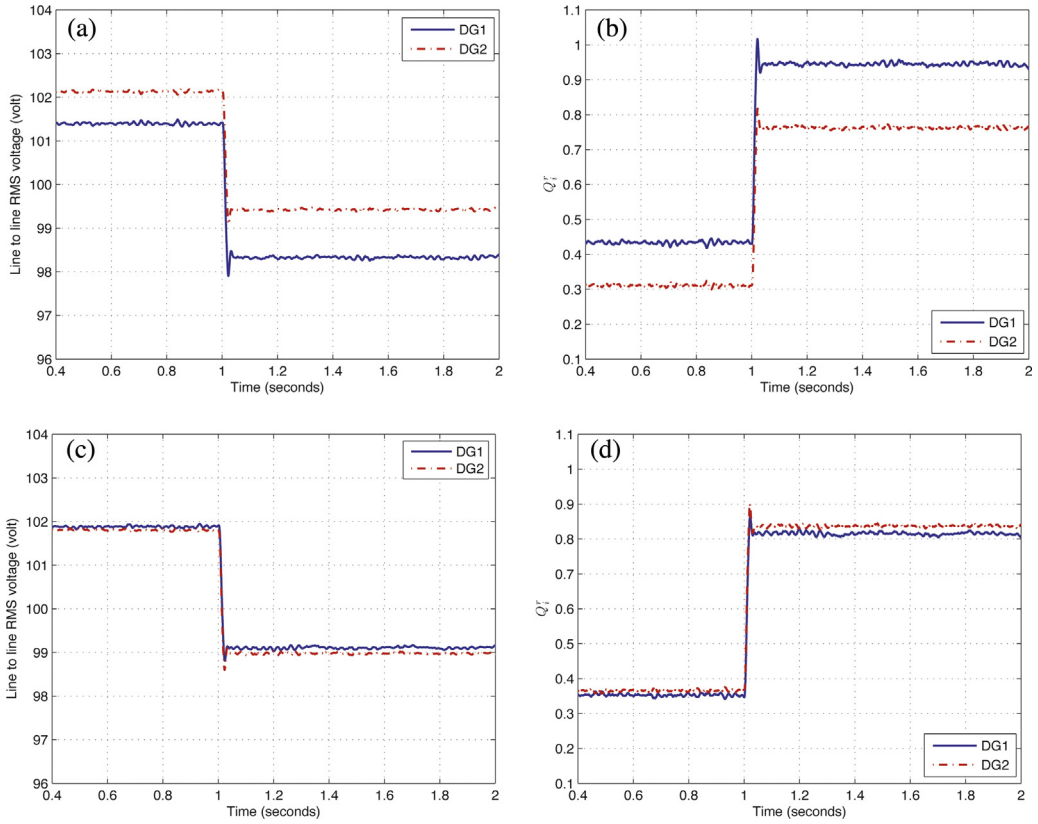

Fig. 4. The reference voltages generated by droop controllers and the ratio Q_i^r, using conventional droop controller and a virtual inductance shown in (a) and (b), and using conventional droop controller combined with our proposed adaptive virtual inductance method shown in (c) and (d).

the DGs. Fig. 4a shows the voltage reference generated by the droop controllers, which are voltages of the sources in the equivalent circuit (E_1, E_{ref}). As observed from the figure, the voltage references created by droop controllers are different, which implies reactive power sharing mismatch among inverters. In this case, an increase in the reactive power demand leads to an increase in the voltage difference of about 1 V as shown in Fig. 4a, where the critical load is doubled at $t = 1$ s.

To show the reactive power sharing deviation caused by voltage differences, we define the following ratio

$$Q_i^r = \frac{Q_i - Q_i^*}{Q_i^{\max} - Q_i^*} \tag{16}$$

Fig. 4b depicts the ratio Q_i^r for the two DGs. An accurate power sharing requires the same value for the two DGs but as shown in Fig. 4b there is a significant reactive power difference among DGs especially when the load increases. As observed from the figure, when the microgrid is highly loaded (after $t = 1$ s), first DG operates very close to its maximum reactive power point while the reference DG is far from its maximum operating point. Hence, a higher increase in load demand causes the first DG to violate it maximum operating point which may lead to its outage.

To cope with the reactive power sharing inaccuracy, the conventional virtual inductance loop is replaced with the proposed method shown in Fig. 2. The reference voltage magnitudes provided by the droop controllers using the proposed adaptive virtual inductance loop are depicted in Fig. 4c. The EMS sends the reference unit parameters given in Table 1 to first DG which changes its inductance value to track the estimated voltage of reference unit's droop control output. As shown in Fig. 4c, the voltage difference between two units is less than 0.15 V for all operating conditions. This difference could be the result of the voltage drops caused by active power and virtual impedance loop inaccuracy introduced by its low pass filter. Comparing the results obtained from the proposed method (Fig. 4c) with those from the conventional virtual inductance approach (Fig. 4a) demonstrates the efficiency of the proposed method to compensate for the voltage drop differences in the microgrids. To observe this, the ratio Q_i^r for the proposed approach is plotted in Fig. 4d. Comparison between the obtained results and those from the conventional method (see Fig. 4b) shows that employing the proposed modified virtual inductance loop improves the reactive power sharing significantly especially under high loads.

As discussed earlier, the proposed adaptive virtual inductance loop can be employed in microgrids with even a large number of different DGs operating in parallel. To illustrate this, two more DGs are added to the simulated microgrid of the previous example. The two new DGs are assumed to have the same parameters as the first DG; however, line reactance of DG3 is considered to be 0.27 mH, and the maximum reactive power and dispatched reactive power in grid-connected mode for DG4 are set to 550 and 75 Var, respectively.

Table 1
The microgrid simulation parameters

Parameter	DG1	Reference DG
Nominal line to line voltage (rms)	104 V	104 V
DG minimum line to line voltage (rms)	98 V	98 V
DG maximum active and reactive power	500 W, 500 Var	500 W, 650 Var
Inverter switching frequency	4500 Hz	4500 Hz
Line resistance and reactance	0.4Ω, 0.3 mH	0.4Ω, 0.6 mH
DC link voltage	230 V	230 V
Output filter inductance and capacitance	5 mH, 40 μF	5 mH, 40 μF
Dispatched powers in grid-connected mode	175 W, 75 Var	175 W, 150 Var
Virtual inductance	Variable	2 mH

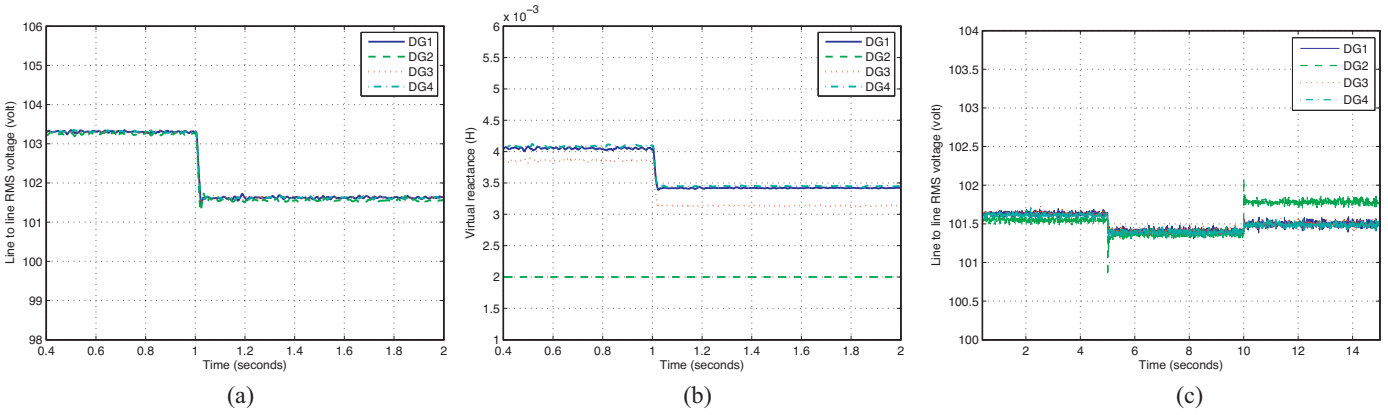

Fig. 5. (a) The reference voltages generated by droop controllers for all four DGs; (b) the values of virtual reactances for DGs using the proposed method; (c) the effects of EMS update and the communication loss on reference voltages generated by droop controllers.

This is to show the ability of the proposed method to achieve reactive power sharing for DGs with even different ratings. As shown in Fig. 5a, all four voltage droops operate at almost same voltage level for all operating conditions, which implies a highly accurate reactive power sharing. Also, the variations of virtual inductances shown in 5b illustrate how our proposed method adapts the inductance value to achieve reactive power sharing among DGs. As shown in this figure, the adaptive virtual inductance loop responds quickly in order to correct the reactive power sharing mismatch after a load change.

Next, we examine the roles of EMS and communication link while the load is considered to be constant. We assume that the update interval for the EMS is 5 s. Fig. 5c shows the reference voltage for all four DGs. At $t = 5$ s, Q^*_{ref} is changed from 150 to 100 Var. EMS sends the change in parameter of reference DG to all DGs via communication link. As observed from Fig. 5c, all the DGs adapt their virtual inductance to generate the same reference voltage, which guarantees an accurate reactive power sharing. At $t = 10$ s, Q^*_2 is changed back to 150 Var, but it is assumed that due to the loss of communication, other DGs do not receive the updated values of reference parameters. Communication loss results in the DGs to estimate the voltage drop of reference DG with error. As illustrated in Fig. 5c, there are now differences between E_{ref} (E_2) and E_1, E_3, E_4. However, all other droops operate at the same voltage level, and so the proposed control strategy is able to continue its operation with only a small reactive power sharing inaccuracy even in the case of a communication loss.

To investigate the effect of the proposed method on circulating current, it is considered that both inverters have the same ratings as the reference DG in Table 1 with the only difference between the two DGs being their line inductances. The circulating currents

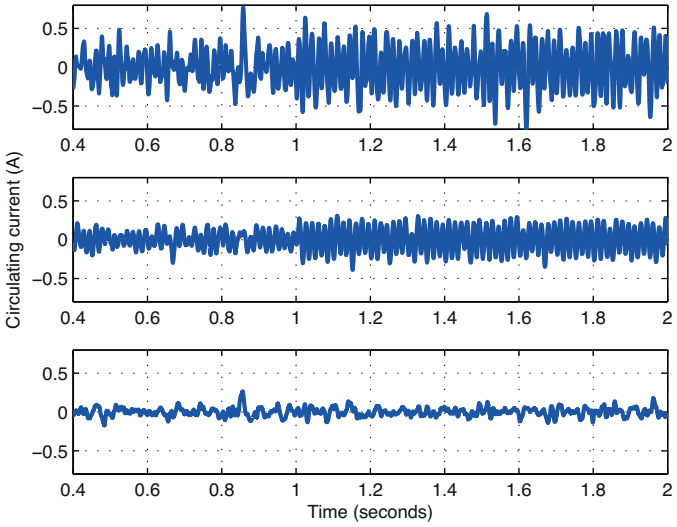

Fig. 6. The circulating current among DGs, with no virtual inductance loop (top plot), with conventional virtual inductance loop (middle plot), and with our proposed approach (bottom plot).

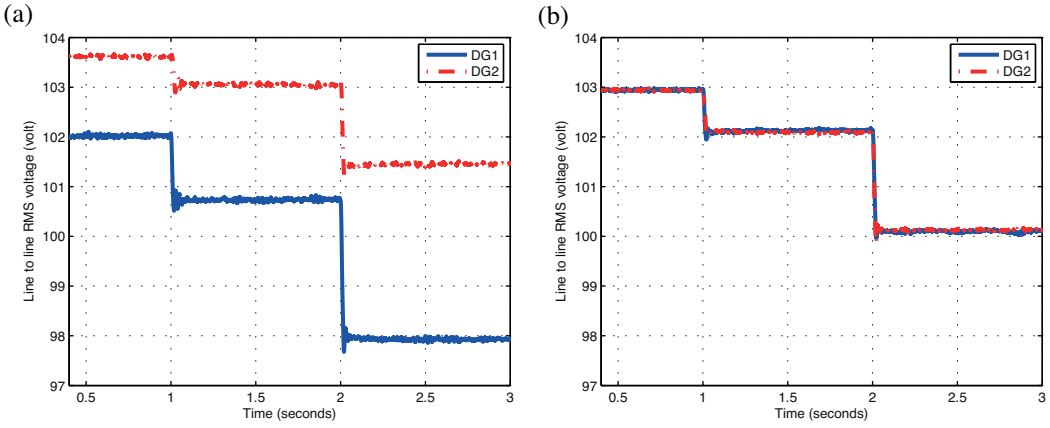

Fig. 7. The reference voltages generated by a conventional droop controller and (a) virtual inductance loop $L_1^{\text{vir}} = 2\,mH$, (b) our proposed modified adaptive virtual inductance loop.

among the inverters for microgrid without virtual inductance, with conventional and proposed virtual inductances are shown in Fig. 6. The first plot shows that there is a high circulating current among the inverters because of voltage differences among two DGs caused by inductance mismatch. Also, small line inductance has intensified the circulating current. The second plot shows the result using traditional virtual inductance loop ($L_1^{vir} = L_2^{vir} = 2\,mH$) as applied in Ref. [12]. The virtual inductance reduces the circulating current because of an increase in the inductance of both inverters but there is still a considerable circulating current due to the voltage mismatch between two voltage sources. Finally, the circulating current after applying the proposed adaptive virtual inductance is shown in the last plot, which illustrates a very small circulating current among DGs because of almost equal voltages at the output of DGs and also large inductance introduced by the virtual inductance loop.

In order to validate the accuracy of the proposed approach to cope with reactive power sharing deviation caused by a local load, we assume that a local load is connected directly to the output of the first DG (see Fig. 3). The voltages E_1 and E_{ref} generated by reactive power droop controller, when the conventional virtual inductance of [7] is used, are illustrated in Fig. 7a. The results show that connecting the local load at $t = 1$ s increases the voltage differences to more than 2 V which results in a poor power sharing among inverters. In addition, the critical load increment ($t = 2$ s) significantly intensifies the reactive power sharing deviation. As shown in Fig. 7a, after $t = 2$ s, the first DG operates below the minimum acceptable voltage, which means that it provides a reactive power higher than its limit, while the second DG is far from its maximum reactive power margin. To address this issue, the modified version of the proposed adaptive virtual inductance loop is employed and the voltage profiles are shown in Fig. 7b. The figure illustrates that the proposed method enables the DGs to track the E_{ref} with very small error for different operating conditions in the presence of local loads only by using local measurement and EMS measurements.

5. Concluding remarks

This paper presents a new droop-based power control strategy to achieve proportional reactive power sharing among DGs. The proposed approach employs an adaptive virtual inductance loop which enables the DGs to track the reference unit voltage magnitude while adding high virtual inductances at the outputs of the DGs to help the low- and medium-voltage microgrids enhance the droop controller transient behavior. The proposed method relies only on the local measurements and the data transmitted by EMS at every update interval through low band communication links that exist in modern microgrids. In addition, because of an almost identical voltage references generated by droop controllers and high virtual inductance at the DGs outputs, the proposed method is able to eliminate circulating current among inverters effectively.

References

[1] M.M. Abdelaziz, E. El-Saadany, Maximum loadability consideration in droop-controlled islanded microgrids optimal power flow, Electr. Power Syst. Res. 116 (2014) 168–179.
[2] F. Katiraei, M. Iravani, P. Lehn, Microgrid autonomous operation during and subsequent to islanding process, IEEE Trans. Power Deliv. 20 (1) (2005) 248–257.
[3] A. Bidram, A. Davoudi, Hierarchical structure of microgrids control system, IEEE Trans. Smart Grid 4 (3) (2012) 1963–1976.
[4] T.B. Lazzarin, G.A.T. Bauer, I. Barbi, A control strategy for parallel operation of single-phase voltage source inverters: analysis, design and experimental results, IEEE Trans. Ind. Electron. 60 (6) (2013) 2194–2204.
[5] E. Serban, H. Serban, A control strategy for a distributed power generation microgrid application with voltage and current controlled source converter, IEEE Trans. Power Electron. 25 (12) (2010) 2981–2992.
[6] A. Mohda, E. Ortjohanna, D. Mortonb, O. Omaric, Review of control techniques for inverters parallel operation, Electr. Power Syst. Res. 80 (12) (2010) 1477–1487.
[7] M.C. Chandorkar, D.M. Divan, R. Adapa, Control of parallel connected inverters in standalone AC supply systems, IEEE Trans. Ind. Appl. 29 (1) (1993) 136–143.
[8] J. Guerrero, L.G. Vicuna, J. Matas, J. Castilla, M. Miret, Output impedance design of parallel-connected UPS inverters with wireless load-sharing control, IEEE Trans. Ind. Electron. 52 (4) (2005) 1126–1135.
[9] J. Simpson-Porco, F. Dorfler, F. Bullo, Synchronization and power sharing for droop controlled inverters in islanded microgrids, Automatica 49 (2013) 2603–2611.
[10] A. Tuladhar, H. Jin, T. Unger, K. Mauch, Control of parallel inverters in distributed AC power systems with consideration of line impedance effect, IEEE Trans. Ind. Appl. 36 (1) (2000) 131–138.
[11] Y. Li, C.N. Kao, An accurate power control strategy for power electronics-interfaced distributed generation units operating in a low-voltage multi bus microgrid, IEEE Trans. Power Electron. 24 (2009) 2977–2988.
[12] W. Yao, M. Chen, J. Matas, Design and analysis of the droop control method for parallel inverters considering the impact of the complex impedance on the power sharing, IEEE Trans. Energy Convers. 58 (2011) 576–588.
[13] Y. Mohamed, M. Ashabani, Adaptive decentralized droop controller to preserve power sharing stability of paralleled inverters in distributed generation microgrid, IEEE Trans. Power Electron. 23 (2008) 2806–2816.
[14] H. Tao, J.L. Duarte, M.A.M. Hendrix, Line-interactive UPS using a fuel cell as the primary source, IEEE Trans. Ind. Electron. 55 (8) (2008) 3012–3021.
[15] J. He, Y.W. Li, Analysis, design and implementation of virtual impedance for power electronics interfaced distributed generation, IEEE Trans. Ind. Appl. 47 (6) (2011) 2525–2538.
[16] J.M. Guerrero, L.G. Vicuna, J. Matas, A wireless controller to enhance dynamic performance of parallel inverters in distributed generation systems, IEEE Trans. Power Electron. 19 (5) (2004) 1205–1213.
[17] M.M. Abdelaziz, H. Farag, E. El-Saadany, Fuel-saving benefit analysis of islanded microgrid central controllers, Electr. Power Syst. Res. 125 (2015) 45–54.
[18] E. Barklund, N. Pogaku, M. Prodanovic, Energy management in autonomous microgrid using stability constrained droop control of inverters, IEEE Trans. Power Electron. 23 (5) (2008) 2346–2352.
[19] L. Asiminoaei, R. Teodorescu, F. Blaabjerg, U. Borup, A digital controlled PV-inverter with grid impedance estimation for ENS detection, IEEE Trans. Power Electron. 20 (6) (2005) 1480–1490.